Detailed study of BBN implications of neutrino oscillation generated neutrino asymmetries in some four neutrino models

R. Foot*
School of Physics, Research Centre for High Energy Physics, The University of Melbourne, Parkville 3052, Australia
(Received 10 June 1999; published 28 December 1999)

We re-examine the evolution of neutrino asymmetries in several four neutrino models. The first case involves the direct creation of L_{ν_e} by $\nu_e \leftrightarrow \nu_s$ oscillations. In the second case, we consider the mass hierarchy $m_{\nu_\tau} \gg m_{\nu_\mu}, m_{\nu_e}, m_{\nu_s}$ where $\nu_\tau \leftrightarrow \nu_s$ oscillations generate a large L_{ν_τ} and some of this asymmetry is converted into L_{ν_e} by $\nu_\tau \leftrightarrow \nu_e$ oscillations. We estimate the implications for BBN for a range of cosmologically interesting δm^2 values. The present paper improves on a previous study by taking into account the finite repopulation rate and the time dependence of the distortions to the neutrino momentum distributions. The treatment of chemical decoupling is also improved.

PACS number(s): 98.80.Hw, 26.35.+c

I. INTRODUCTION

If light sterile neutrinos exist, then this will lead to important implications for early Universe cosmology. This is because ordinary-sterile neutrino oscillations generate large neutrino asymmetries for a large range of parameters [1–6]. This is a generic feature of ordinary-sterile neutrino oscillations.

The implications of this phenomena are quite model dependent. Various implications of this phenomena have been discussed in a number of previous papers for a number of interesting models motivated by the existing neutrino anomalies [2–9]. For example in Refs. [2,4,6] it has been shown that the maximal $\nu_\mu \rightarrow \nu_s$ oscillation solution to the atmospheric neutrino anomaly is consistent with a stringent big bang nucleosynthesis (BBN) bound of $N_{eff}^{BBN} \lesssim 3.6$ (and may also be consistent with $N_{eff}^{BBN} < 3$ depending on the model [3,9]). This consistency requires $m_{\nu_\tau} \gtrsim$ few eV (for $|\delta m^2_{atmos}| \simeq 3 \times 10^{-3}$ eV^2), thus placing the ν_τ in the interesting hot dark matter range. Of course this is also of great interest to short-base-line experimentalists.

Of particular concern to this paper is the ''low temperature'' evolution of neutrino asymmetries which also has important implications for BBN. In Ref. [3], we discussed the four neutrino model with $m_{\nu_\tau} \gg m_{\nu_\mu}, m_{\nu_e}, m_{\nu_s}$. In this case a large L_{ν_τ} asymmetry is generated by $\nu_\tau \leftrightarrow \nu_s$ oscillations, some of which is transferred to L_{ν_e} by $\nu_\tau \leftrightarrow \nu_e$ oscillations. This has important implications for BBN since it allows $N_{eff}^{BBN} < 3$, with $N_{eff}^{BBN} \approx 2.5$ for a large range of parameters if $L_{\nu_e} > 0$. Qualitatively similar results occur for other sterile neutrino models as has been shown in a number of recent papers [7,9]. One point of all this is that $N_{eff}^{BBN} < 3$ is a serious possibility if light effectively sterile neutrinos exist.

In Ref. [3] we considered the case of large $|\delta m^2|$ where the L_{ν_e} was created above 1.5–2.0 MeV, so that its implications for BBN could be approximately discussed by using thermal neutrino distributions (i.e. the neutrino asymmetry was distributed with chemical potentials) which were approximately constant during the era when the neutron/proton ratio was changing (i.e. for $T \lesssim 2$ MeV). We also briefly estimated the effects for the direct production of L_{ν_e} by $\nu_e \rightarrow \nu_s$ oscillations (this case is only possible if the other neutrinos are lighter or do not oscillate into the sterile neutrino).

Recently, Ref. [3] has been criticized in Ref. [10] where it is claimed that the time dependence of the neutrino asymmetry and finite repopulation rate (which was assumed to be instantaneous in Ref. [3] for temperatures above about 1.5 MeV) are of critical importance. Reference [10] also similarly criticizes Ref. [7] (which studied a quite different 4 neutrino model with approximately degenerate ν_μ, ν_τ states) but this is clearly unjustified because Ref. [7] takes into account the finite repopulation rate using a Pauli-Boltzman approach (as well as the time dependence of the distortion in the neutrino distributions). In fact, Ref. [10] appears to follow the repopulation procedure advocated in Ref. [7] and re-examines the cases in Ref. [3] using this repopulation procedure. In view of this, we have also decided to revisit the models considered in Ref. [3] in this paper because we believe that the results of Ref. [10] to be incorrect. We will compute the evolution of the number distributions, taking into account the finite repopulation rate and time dependence of the asymmetry. As already emphasized above, such an approach was already used in Refs. [7,9] discussing different models, so it is straightforward to apply it here. We will also improve on Ref. [3] by discussing more completely the effects of the two similar oscillation modes, $\nu_\tau \leftrightarrow \nu_\mu, \nu_\tau \leftrightarrow \nu_e$. We also give a more accurate treatment of the kinetic decoupling region which suggests a slightly lower kinetic decoupling temperature.

II. BIG BANG NUCLEOSYNTHESIS

The primordial deuterium to hydrogen (D/H) ratio can be used to give a sensitive determination of the baryon to photon ratio η which, given the estimated primordial ^{4}He mass fraction, can be used to infer the effective number of light neutrino flavors, N_{eff}^{BBN}, during the BBN epoch. This value can then be compared with the predictions for N_{eff}^{BBN} from various models of particle physics to find out which ones are compatible with standard BBN. For example, the minimal

*Email address: foot@physics.unimelb.edu.au

standard model predicts $N_{eff}^{BBN}=3$. At the present time, most estimates favor $N_{eff}^{BBN}<3.6$ and some estimates favor $N_{eff}^{BBN}<3.0$ [11]. Of course, even if a model of particle physics is shown to be incompatible with BBN, this does not necessarily mean that the model is incorrect, since, for example, it is also possible that one of the standard assumptions of BBN may not be correct [12].

For gauge models with effectively sterile neutrinos, one in general expects $N_{eff}^{BBN}\neq 3$. In fact, N_{eff}^{BBN} may be less than 3 or greater than 3. The prediction for N_{eff}^{BBN} depends on the oscillation parameters in a given model and also the sign of the asymmetry (which for various reasons cannot be predicted at the moment). One possible consequence of ordinary-sterile neutrino oscillations is the excitation of sterile neutrino states, which typically leads to an increase in the expansion rate of the universe and thereby also increases N_{eff}^{BBN}. Another possible consequence of ordinary-sterile neutrino oscillations is the dynamical generation of an electron-neutrino asymmetry. This also has important implications for BBN, as it directly affects the reaction rates which determine the neutron to proton (n/p) ratio just before nucleosynthesis. If the electron neutrino asymmetry is positive, then it will decrease N_{eff}^{BBN}, while if it is negative, then it will increase N_{eff}^{BBN}.

The neutron to nucleon ratio, $X_n(t)$, is related to the primordial Helium mass fraction, Y_P, by[1]

$$Y_P \simeq 2X_n \tag{1}$$

just before nucleosynthesis. The evolution of $X_n(t)$ is governed by the equation,

$$\frac{dX_n}{dt} \simeq -\lambda(n\to p)X_n + \lambda(p\to n)(1-X_n), \tag{2}$$

where the reaction rates are approximately

$$\begin{aligned}\lambda(n\to p) &= \lambda(n+\nu_e \to p+e^-) + \lambda(n+e^+ \to p+\overline{\nu_e}) \\ &\quad + \lambda(n\to p+e^- +\overline{\nu_e}), \\ \lambda(p\to n) &= \lambda(p+e^- \to n+\nu_e) + \lambda(p+\overline{\nu_e}\to n+e^+) \\ &\quad + \lambda(p+e^- +\overline{\nu_e}\to n).\end{aligned} \tag{3}$$

These reaction rates depend on the momentum distributions of the species involved. The 2-body processes in Eq. (3) for determining $n\leftrightarrow p$ are only important for temperatures above about 0.4 MeV. Below this temperature these weak interaction rates freeze out and neutron decay becomes the dominant factor affecting the n/p ratio. For example, an excess of ν_e over $\overline{\nu_e}$, due to the creation of a positive L_{ν_e}, would change the rates for the processes in Eq. (3). The effect of this would be to reduce the n/p ratio, and hence reduce Y_P. Neutron decay is not significantly altered by lepton asymmetries unless they are very large. It is quite well known that a small change in Y_P due to the modification of ν_e and $\overline{\nu_e}$ distributions does not impact significantly on the other light element abundances (see for example Ref. [14]). A small modification to the expansion rate, using the convenient unit N_{eff}^{BBN}, primarily affects only Y_P, with[2] [15]

$$\delta Y_P \simeq 0.012\times \delta N_{eff}^{BBN}. \tag{4}$$

Since Appendix A of Ref. [9] describes in detail how we compute the effect on Y_P due to the modified ν_e and $\overline{\nu_e}$ distributions, we will not discuss it further here.

III. CASE 1: IMPLICATIONS FOR BBN OF $\nu_e \leftrightarrow \nu_s$ OSCILLATION GENERATED L_{ν_e}

In this section we will study the direct production of a large L_{ν_e} from $\nu_e\leftrightarrow\nu_s$ oscillations. We will ignore oscillations involving ν_μ or ν_τ. This is only an approximately valid thing to do provided that either their masses are very small (so that the largest $|\delta m^2|$ belongs to the $\nu_e\leftrightarrow\nu_s$ oscillations and the other oscillations have $|\delta m^2|$ much less than 1 eV^2) *or* that they do not mix with the ν_e,ν_s (i.e. the ν_e,ν_s decouple from the ν_μ,ν_τ in the neutrino mass matrix).

Let us begin with some necessary preliminaries. Our notation and convention for ordinary-sterile neutrino two state mixing is as follows. The weak and sterile eigenstates ν_α $(\alpha=e,\mu,\tau)$ and ν_s are linear combinations of two mass eigenstates ν_a and ν_b,

$$\nu_\alpha = \cos\theta_{\alpha s}\nu_a + \sin\theta_{\alpha s}\nu_b, \quad \nu_s = -\sin\theta_{\alpha s}\nu_a + \cos\theta_{\alpha s}\nu_b, \tag{5}$$

where $\theta_{\alpha s}$ is the vacuum mixing angle. We define $\theta_{\alpha s}$ so that $\cos 2\theta_{\alpha s}>0$ and we adopt the convention that $\delta m_{\alpha s}^2 \equiv m_b^2 - m_a^2$.

Recall that the α-type neutrino asymmetry is defined by

$$L_{\nu_\alpha} \equiv \frac{n_{\nu_\alpha} - n_{\overline{\nu}_\alpha}}{n_\gamma}. \tag{6}$$

In the above equation, n_γ is the number density of photons, $n_\gamma = 2\zeta(3)T^3/\pi^2$. Note that when we refer to ''neutrinos,'' sometimes we will mean neutrinos and/or antineutrinos. We hope the correct meaning will be clear from the context. Also, if neutrinos are Majorana particles, then technically they are their own antiparticle. Thus, when we refer to ''antineutrinos'' we obviously mean the right-handed helicity state in this case.

In Ref. [1] it was shown that ordinary-sterile neutrino oscillations generate large neutrino asymmetries for a wide range of parameters. This work built upon earlier work on

[1]For a review of helium synthesis, see for example Ref. [13].

[2]Note that several authors prefer to use δY_P rather than δN_{eff}^{BBN}. The difference is essentially a matter of convention since these two quantities are approximately related by Eq. (4).

ordinary-sterile neutrino oscillations in the early Universe [18]. Large asymmetry generation occurs for the parameter region [2,3]

$$\delta m^2_{\alpha s} < 0 \quad \text{with} \quad |\delta m^2_{\alpha s}| \lesssim 10^{-4} \ \text{eV}^2,$$
$$\text{few} \times 10^{-10} \lesssim \sin^2 2\theta_{\alpha s} \lesssim \text{few} \times 10^{-5} \left(\frac{\text{eV}^2}{|\delta m^2_{\alpha s}|} \right)^{1/2}. \tag{7}$$

The upper bound on $\sin^2 2\theta_{\alpha s}$ in the above equation comes from the constraint that $\nu_\alpha \leftrightarrow \nu_s$ oscillations do not populate the sterile states at high temperatures before the neutrino asymmetry is initially generated, i.e. for $T \gtrsim T_c$ [2,6]. Note that in the present paper we limit ourselves to the above region of parmeters. For completeness let us mention that for $|\delta m^2| \ll 10^{-4}$ eV^2, the lepton number generation is much smaller, typically much less than about 10^{-7} according to Refs. [16].[3] Apparently this can still affect BBN indirectly for a window of parameters with $|\delta m^2_{es}| \sim 10^{-8}$ eV^2 [17].

As already discussed in detail in previous publications [3,2,1] the evolution of lepton number can be separated into three distinct phases. At high temperatures the oscillations are damped and evolve so that $L^{(\alpha)} \to 0$ (where $L^{(\alpha)} \equiv L_{\nu_\alpha} + L_{\nu_e} + L_{\nu_\mu} + L_{\nu_\tau} + \eta$, and η is related to the baryon asymmetry). In this region the resonance momentum for neutrino oscillations is approximately the same as anti-neutrino oscillations. If $\delta m^2_{\alpha s} < 0$, then at a certain temperature, T_c, which is given roughly by [1]

$$T_c \sim 16 \left(\frac{-\delta m^2_{\alpha s} \cos 2\theta_{\alpha s}}{\text{eV}^2} \right)^{1/6} \text{MeV}, \tag{8}$$

exponential growth of neutrino asymmetry occurs (which typically generates a neutrino asymmetry of order 10^{-5} at $T \simeq T_c$; see Fig. 1 of Ref. [4] for some typical examples). Taking for definiteness that the L_{ν_α} is positive, the anti-neutrino oscillation resonance moves to very low values of $p/T \sim 0.3$ while the neutrino oscillation resonance moves to high values $p/T \gtrsim 10$ (see Ref. [3] for a figure illustrating this). The subsequent evolution of neutrino asymmetries, which is dominated by adiabatic Mikheyev-Smirnov-Wolfenstein (MSW) transitions of the antineutrinos, follows an orderly $1/T^4$ behavior until the antineutrino resonance has passed through the entire distribution. The final asymmetry generated is typically in the range $0.23 \lesssim L_{\nu_\alpha} \lesssim 0.37$ [3]. Because the oscillations are dominated by adiabatic MSW behavior, it is possible to use a relatively simple and accurate formalism to describe the evolution of the system at the ''low temperatures,'' $T \lesssim T_c/2$. In fact, we only need to know the values of the oscillation resonance momentum at $T \simeq T_c/2$. Previous numerical work has already shown [3] that by $T \simeq T_c/2$, neutrino asymmetry is generated such that $0.2 \lesssim p/T \lesssim 0.8$ (the precise value depends on $\sin^2\theta_{\alpha s}, \delta m^2_{\alpha s}$). Furthermore, the subsequent evolution is approximately insensitive to the initial value of p/T in this range (provided, of course, that negligible number of sterile neutrinos were produced at high temperature).

In this section we will deal with the case of $\nu_e \leftrightarrow \nu_s$ oscillations directly producing the L_{ν_e} asymmetry. For the implications for BBN we are primarily interested in the ''low temperature'' evolution of the number distributions and lepton numbers in this case. Our analysis can be broken up into the following steps:

(1) We assume complete adiabatic MSW conversion of neutrinos at the MSW resonance.

(2) From this we can compute the evolution of lepton number asymmetries which not only dictates the momentum of the MSW resonances, but also the chemical potentials.

(3) Using these chemical potentials we can evaluate the equilibrium distributions from which we can estimate the actual distributions by a Pauli-Boltzman repopulation equation.

We now discuss each of these steps in detail.

Consider, for the moment, two-flavor small angle (i.e. $\cos 2\theta_{es} \simeq 1$) ordinary-sterile $\nu_e \leftrightarrow \nu_s$ neutrino oscillations. As discussed in detail in earlier papers the $\nu_e \leftrightarrow \nu_s$ neutrino oscillations only generate L_{ν_e} provided that $\delta m^2_{es} < 0$ and this will be assumed in the forthcoming discussion.[4] We know from numerical integration of the exact quantum kinetic equations [3] that the adiabatic approximation is valid provided that $\sin^2 2\theta_{es} \gtrsim \text{few} \times 10^{-10}$. Now, coherent small angle adiabatic MSW transitions completely convert $\nu_e \leftrightarrow \nu_s$ at the resonance momentum of these states. The resonance momentum is given approximately by (see e.g. Ref. [3]),

$$\frac{p_{res}}{T} = \frac{|\delta m^2_{es}|}{a_0 T^4 L^{(es)}}, \tag{9}$$

where $a_0 \equiv 4\sqrt{2}\zeta(3) G_F/\pi^2$ and

$$L^{(es)} \equiv 2L_{\nu_e} + L_{\nu_\tau}. \tag{10}$$

In the above equation we have neglected the L_{ν_μ} asymmetry (as well as the baryon-electron asymmetry). This is because these asymmetries are unimportant in the low temperature region unless they happen to be large (i.e. greater than about 10^{-5}). For adiabatic two-flavor neutrino oscillations in the early Universe it is quite easy to see that the rate of change of lepton number is governed by the simple equation [3]

$$\frac{dL_{\nu_e}}{dT} = -X(p_{\text{res}}) \left| \frac{d(p_{\text{res}}/T)}{dT} \right|, \tag{11}$$

[3]For the historical record, the reader should be aware that Refs. [16] also argued that neutrino asymmetry was always small (less than 10^{-7}) and unimportant for all parameters of interest in contrast to the later studies of Refs. [1–5].

[4]Note that $|\delta m^2_{es}| \lesssim m^2_{\nu_e}$ (where m_{ν_e} is the mass of the state which is predominately ν_e). Recall that there is an experimental upper bound on m_{ν_e} which is a few eV if ν_e is a Dirac neutrino and about 1 eV if ν_e is a Majorana neutrino [19].

where $p_{\rm res}$ is the MSW resonance momentum, Eq. (9), and

$$X(p)=\frac{T}{n_\gamma}[N^-_{\nu_e}(p)-N^-_{\nu_s}(p)]. \tag{12}$$

Also, $N^-_{\nu_e}(p)$ and $N^-_{\nu_s}(p)$ are the momentum distributions of the $\overline{\nu}_e$ and $\overline{\nu}_s$ states. In the above equations, the case $L_{\nu_e}>0$ has been considered (so that the resonance occurs for antineutrinos). Equation (11) relates the rate of change of lepton number to the speed of the resonance momentum through the neutrino distribution. Reference [5] provides a detailed discussion of how this equation can be derived from the quantum kinetic equations for the case of adiabatic evolution with a narrow resonance width. As discussed in Ref. [3], Eq. (11) can be simplified using

$$\frac{d(p_{\rm res}/T)}{dT}=\frac{\partial(p_{\rm res}/T)}{\partial T}+\frac{\partial(p_{\rm res}/T)}{\partial L_{\nu_e}}\frac{dL_{\nu_e}}{dT}, \tag{13}$$

from which it follows that

$$\frac{dL_{\nu_e}}{dT}=\frac{fX\dfrac{\partial(p_{\rm res}/T)}{\partial T}}{1-fX\dfrac{\partial(p_{\rm res}/T)}{\partial L_{\nu_e}}}=\frac{-4fXp_{\rm res}}{T^2+\dfrac{2fTXp_{\rm res}}{L^{(es)}}}, \tag{14}$$

where $f=1$ for $d(p_{\rm res}/T)/dt>0$ [that is for $d(p_{\rm res}/T)/dT<0$] and $f=-1$ for $d(p_{\rm res}/T)/dt<0$ and we have dropped the momentum dependence of X in the above equation for notational clarity.[5] Equation (14) allows us to compute the evolution of L_{ν_e}. As discussed earlier, it is valid from $T\simeq T_c/2$ (with $p_{res}/T\sim 0.3$ at this point). For the more complicated multi-flavor case considered in Sec. IV, coupled equations based on Eq. (14) will be used. We now must describe how we compute the evolution of N_{ν_α}.

The MSW transitions effect the adiabatic conversion

$$|\overline{\nu}_e\rangle\leftrightarrow|\overline{\nu}_s\rangle. \tag{15}$$

This means that as P_1 sweeps through the $\overline{\nu}_e$ momentum distribution,

$$N^-_{\nu_s}(P_1)\rightarrow N^-_{\nu_e}(P_1),$$

$$N^-_{\nu_e}(P_1)\rightarrow N^-_{\nu_s}(P_1). \tag{16}$$

In our numerical work the continuous momentum distribution for each flavor is replaced by a finite number of ''cells'' on a logarithmically spaced mesh. As the momentum P_1 passes a cell, the number density in the cell is modified according to Eq. (16). Of course weak interactions will repopulate some of these cells as they thermalize the neutrino momentum distributions. The repopulation can also generate small chemical potentials for the other flavors (as will be discussed later). We take repopulation into account with the rate equation for each flavor $\alpha=e,\mu,\tau$,

$$\frac{\partial}{\partial t}\frac{N_{\nu_\alpha}(p)}{N_0(p,T)}\simeq\Gamma_\alpha(p)\left[\frac{N^{\rm eq}(p,T,\mu_{\nu_\alpha})}{N_0(p,T)}-\frac{N_{\nu_\alpha}(p)}{N_0(p,T)}\right],$$

$$\frac{\partial}{\partial t}\frac{N^-_{\nu_\alpha}(p)}{N_0(p,T)}\simeq\Gamma_\alpha(p)\left[\frac{N^{\rm eq}(p,T,\overline{\mu}_{\nu_\alpha})}{N_0(p,T)}-\frac{N^-_{\nu_\alpha}(p)}{N_0(p,T)}\right], \tag{17}$$

where $\Gamma_\alpha(p)$ is the total collision rate and is approximately given by

$$\Gamma_\alpha(p)=y_\alpha G_F^2T^5\left(\frac{p}{3.15T}\right), \tag{18}$$

with $y_e\simeq 4.0, y_{\mu,\tau}\simeq 2.9$ and G_F is the Fermi constant. Also, in Eq. (17), $N_0(p,T)$, $N^{eq}(p,T,\mu_{\nu_\alpha})$ are the equilibrium distributions with zero chemical potential and chemical potential μ_{ν_α} respectively.[6] Previous papers [7,9] used a simple approximation whereby the transition out of chemical equilibrium occurred at the decoupling temperature T^α_{dec}. Obviously this is not a sharp transition. Also, there will be small chemical potentials created by the other flavors as they create $\overline{\nu}_e\nu_e$ pairs to compensate for the loss of $\overline{\nu}_e$ states. In the Appendix we discuss a more accurate (but more complicated) formalism to compute the values of the chemical potentials for all of the flavors as a function of time (or equivalently temperature). The conclusion is that the simple treatment of chemical decoupling, discussed in previous papers, is roughly valid, but noticable differences (though typically not greater than about $\delta N^{BBN}_{eff}\sim 0.2$) for BBN can occur. [Although there will not be much difference for the $\nu_e\leftrightarrow\nu_s$ case since the lepton number is generated so late, since experimentally $|\delta m^2_{es}|\lesssim 10$ eV^2 (see footnote 2)]. We will use the more complicated formalism discussed in the Appendix to evaluate the chemical potentials for all of our numerical work in this paper.

Using the above procedure the lepton asymmetry L_{ν_e} and the neutrino distributions $N_{\nu_\alpha}(p,t), N^-_{\nu_\alpha}(p,t)$ can be obtained. We can feed the $N_{\nu_e}(p,t), N^-_{\nu_e}(p,t)$ distributions into a nucleosynthesis code (which we integrate concurrently) in order to compute the implications for BBN. It is useful to separate the total contribution to δY_P into two contributions,

$$\delta Y_P=\delta_1 Y_P+\delta_2 Y_P, \tag{19}$$

where $\delta_1 Y_P$ is the change due to the effect of the modified electron neutrino momentum distributions on the nuclear reaction rates, and $\delta_2 Y_P$ is due to the change in the energy density (or equivalently the change in the expansion rate of the universe). While BBN is only sensitive (to a good ap-

[5]At $T=T_c/2$, $f=1$ and it does not change sign during subsequent evolution.

[6]Our convention for the sign of the chemical potential is $N^{eq}(p,T,\mu_{\nu_\alpha})=(1/2\pi^2)p^2/1+e^{(p+\mu_{\nu_\alpha})/T}$.

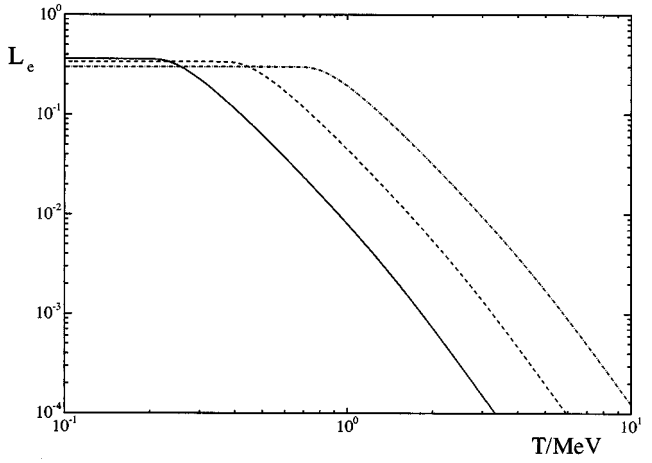

FIG. 1. Low temperature evolution of L_{ν_e}/h ($h \equiv T_\nu^2/T_\gamma^3$) due to $\nu_e \leftrightarrow \nu_s$ oscillations, for the parameter choices, $\delta m^2 = -0.1$ eV^2 (solid line), $\delta m^2 = -1$ eV^2 (dashed line) and $\delta m^2 = -10$ eV^2 (dash-dotted line).

proximation) to the total contribution, δY_P, the separate parts will have quite different implications for the forthcoming precision measurements of the anisotropy of the cosmic microwave background. In particular it may be possible to estimate the expansion rate of the Universe at the time of photon decoupling [21].

The contribution $\delta_1 Y_P$ can be determined by numerically integrating the rate equations for the processes given in Eq. (3) using the modified electron neutrino momentum distributions N_{ν_e} and $N_{\bar{\nu}_e}$ as discussed in Appendix A of Ref. [9]. The contribution $\delta_2 Y_P$ can be computed from the momentum distributions of the ordinary and sterile neutrinos through

$$\delta_2 Y_P \simeq 0.012 \left(\frac{1}{2\rho_0} \int_0^\infty \left[N_{\bar{\nu}_s}(p) + \sum_{\alpha=1}^{3} N_{\nu_\alpha}(p) + N_{\bar{\nu}_\alpha}(p) \right] p\,dp - 3 \right), \qquad (20)$$

where

$$\rho_0 \equiv \int_0^\infty N_0(p,T)\,p\,dp = \frac{7\pi^2}{240} T^4 \qquad (21)$$

is the energy density of a Weyl fermion at equilibrium with zero chemical potential. [Recall that Eq. (4) can be used to express δY_P, $\delta_1 Y_P$ and $\delta_2 Y_P$ in terms of effective neutrino number, δN_{eff}^{BBN}, $\delta_1 N_{eff}^{BBN}$ and $\delta_2 N_{eff}^{BBN}$, respectively.] To calculate $\delta_2 Y_P$, we numerically determine the momentum distributions at $T = 0.5$ MeV. Because of the approximate kinetic decoupling of neutrinos for temperatures below about 3 MeV, large contributions[7] to $\delta_2 Y_P$, should they exist, must have been generated earlier. A temperature of 0.5 MeV is therefore a safe place to evaluate the final $\delta_2 Y_P$.

Recall that there is an ambiguity concerning the sign of the L_{ν_e} lepton asymmetry. We have considered the $L_{\nu_e} > 0$ case above for definiteness, but $L_{\nu_e} < 0$ is equally likely *a priori*. Previous work [2] has shown that the sign is fixed in the region where the ''static approximation'' is valid. This approximation assumes that the asymmetry evolution is dominated by collisions and is sufficiently smooth.[8] Importantly it is generally valid in the region $T \simeq T_c$ where the neutrino asymmetry is initially generated provided that $\sin^2 2\theta \lesssim \mathcal{O}(10^{-6})$ [2] for $\delta m^2 \sim -10$ eV^2. Thus in this region of parameters the sign is fixed. For $\sin^2 2\theta \gtrsim \mathcal{O}(10^{-6})$ numerical integration of the quantum kinetic equations (including the momentum distribution of the neutrinos) reveals [4] that the sign oscillates[9] for a short period at $T \simeq T_c$. In the parameter region where the sign oscillates (and possibly in some of the parameter region where it does not oscillate) the sign may not be fixed when fluctuations are considered [24]. It may be possible for different regions of space to have different signs of the lepton number, as first suggested in Ref. [1]. Whether this happens or not is an open question at the moment and will depend on the size of the fluctuations present.

In any case, even if the sign is fixed, it cannot be predicted as it depends on the initial values of the neutrino asymmetries (as well as the baryon asymmetry). For the negative L_{ν_e} case, the roles of particles and anti-particles are reversed. One consequence of this is that the signs of all the other asymmetries are also reversed. The quantity $\delta_1 Y_P$ will obviously be significantly affected by this ambiguity in sign, while $\delta_2 Y_P$ will not be affected at all. This means that we have two possible values for the overall change in the effective number of neutrino flavors during BBN. The results of the numerical work is presented in Figs. 1–3. In Fig. 1 we show the evolution of L_{ν_e} for three examples, $\delta m_{es}^2/\text{eV}^2 = -0.1, -1, -10$. We emphasize that the evolution is approximately independent of $\sin^2 2\theta_{es}$ as long as $\sin^2 2\theta_{es}$ is in the range given in Eq. (7). As explained earlier, we start the low temperature evolution at $T \sim T_c/2$ with the value of p_{res}/T

[7] By ''large contributions'' we mean $\delta_2 N_{eff}^{BBN} \gtrsim 0.10$.

[8] In fact, it has been shown in Ref. [5] that this approximation is equivalent to the adiabatic limit of the quantum kinetic equations in the region where collisions dominate the evolution of the neutrino asymmetry.

[9] Note that the recent study in Ref. [22], which neglects the neutrino momentum distribution, arrives at quite different results. They find that the region where the sign does not oscillate is much smaller, roughly, $\sin^2 2\theta \lesssim \mathcal{O}(10^{-8})$ for $\delta m^2 \sim -10$ eV^2. Qualitatively, this is very easy to understand. The reason is that in the average momentum toy model, all of the neutrinos enter the MSW resonance at the same time which significantly enhances the rate at which neutrino asymmetry is created at $T = T_c$. The rapid creation of neutrino asymmetry reduces the region where the oscillations are adiabatic [2]. Also, the paper in Ref. [23] similarly assumes that all of the neutrinos have the same momentum, but (perhaps not surprisingly) obtain quite different results from Ref. [22].

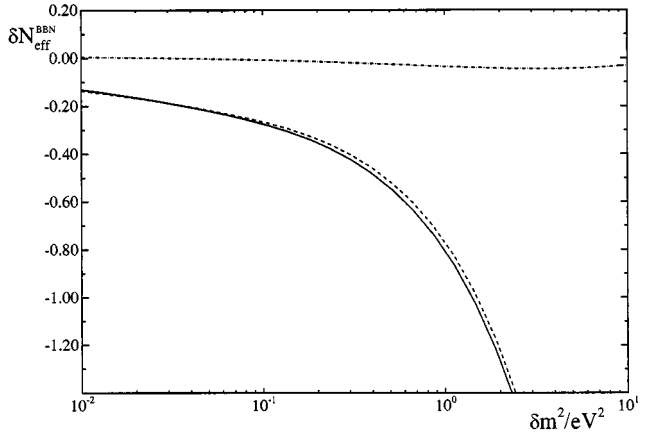

FIG. 2. δN_{eff}^{BBN} versus $|\delta m_{es}^2|$. The dashed line is the contribution $\delta_1 N_{eff}^{BBN}$ due to the effects of the L_{ν_e} asymmetry while the dash-dotted line is the contribution $\delta_2 N_{eff}^{BBN}$ due to the change in the expansion rate. The solid line is the total contribution $\delta N_{eff}^{BBN} = \delta_1 N_{eff}^{BBN} + \delta_2 N_{eff}^{BBN}$. This figure considers the case $L_{\nu_e} > 0$.

~ 0.3. Of course the full evolution from $T \gg T_c$ to $T \to 0$ can be obtained from numerical integration of the quantum kinetic equations (see e.g. Ref. [4]). However, for the applications considered in this paper only the low temperature evolution is required, which is why we use the much simpler formalism based on Eq. (14).

The implications for BBN are shown in Figs. 2 and 3. Figure 2 treats the $L_{\nu_e} > 0$ case, while Fig. 3 displays the $L_{\nu_e} < 0$ case. As these figures show, the effect of the $\nu_e \leftrightarrow \nu_s$ oscillations on BBN is very significant and depends sensitively on the sign of the asymmetry and on the δm_{es}^2 value. We emphasize that our equations contain approximations. The most important are that the repopulation is handled approximately via Eq. (17). It is obviously difficult to estimate the size of this uncertainty without computing repopulation exactly. Nevertheless, we expect that this theoretical uncertainty is typically less than $\delta N_{eff}^{BBN} \sim 0.2$.

It is evident that $\delta_2 Y_P$ is close to zero for the range of δm_{es}^2 considered. This can be approximately understood by noting that the generation of sterile states occurs below the kinetic decoupling temperature for ν_e's. This means that the

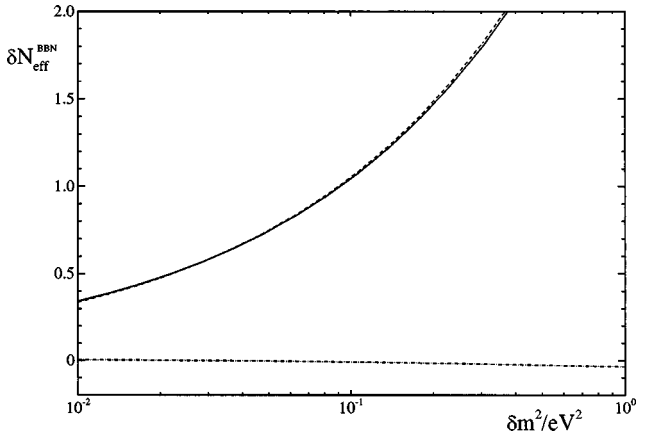

FIG. 3. Same as Fig. 2 except $L_{\nu_e} < 0$ is considered.

ν_e states which have been converted into sterile states are not replaced. Note that the kinetic decoupling rate is governed by the *inelastic* collision rate of the ν_e's. However, it is important to understand that the elastic collision rate is nearly an order of magnitude larger than the inelastic collision rate. The effect of the elastic collisions is to modify the momentum distribution of the neutrinos such that they approach a thermal distribution. Note that while the elastic collisions do not change the total number of ν_e states they do modify the momentum distribution and thus can slightly affect the energy density (or, more correctly, energy density/T^4). It is this thermalization effect which is responsible for the slightly negative value of $\delta_2 Y_P$ for $\delta m_{es}^2 \sim$ few eV^2. Indeed, as the MSW resonance moves through the low momentum part of the spectrum the MSW transitions deplete the $\overline{\nu}_e$'s before the $\overline{\nu}_e$ spectrum is significantly distorted by the L_{ν_e} asymmetry. However, by the time p/T moves to the higher momentum part (i.e. $p/T \gtrsim 4$), the neutrino asymmetry is so large that the number of $\overline{\nu}_e$ states are significantly reduced (cf. with the Fermi-Dirac distribution with zero chemical potential). For this reason the oscillations deplete more low momentum neutrinos than high momentum ones. The concurrent thermalization of the neutrino distribution evidently reduces the average p/T per neutrino, and hence the energy density *divided by* T^4 can be slightly reduced. Of course the temperature of the $\overline{\nu}_e$ states would be expected to increase a little, which in our approximation is neglected (much of this temperature increase would be absorbed by the other flavors which are still in approximate thermal equilibrium down to temperatures 1–2 MeV).

Note that in the case of very small $|\delta m_{es}^2|/\text{eV}^2 \sim 10^{-2}$, the dominant effect of the neutrino asymmetry in the $L_{\nu_e} > 0$ case is the modification to the Pauli blocking of the neutron decay. Ordinarily neutrino asymmetries lead to a negligible effect for neutron decay; however, in this case the effect is small (but not completely negligible) because the neutrino asymmetry is so large ($L_{\nu_e} \simeq 0.37$ for $\delta m_{es}^2/\text{eV}^2 \sim -10^{-2}$).

Finally note that our results are quite different to the results of Ref. [10]. We do not know why this is the case. Unfortunately, Ref. [10] gives few details of how they computed the evolution of the neutrino asymmetry. Thus it is difficult to know whether the difference lies in the details of the asymmetry evolution or in the BBN code.

This concludes our study of the direct production of L_{ν_e} from $\nu_e \leftrightarrow \nu_s$ oscillations. We now consider the alternative, but more complicated case of the indirect production of L_{ν_e} from a large L_{ν_τ} asymmetry.

IV. CASE 2: IMPLICATIONS FOR BBN IN THE FOUR NEUTRINO SCENARIO WITH $M_{\nu_\tau} \gg M_{\nu_\mu}, M_{\nu_e}, M_{\nu_s}$

We now discuss the second scenario of Ref. [3], that is a four neutrino model with

$$m_{\nu_\tau} \gg m_{\nu_\mu}, m_{\nu_e}, m_{\nu_s}. \tag{22}$$

We will first deviate from Ref. [3] by considering the simpler case where the muon neutrino is ignored. Strictly, this would only be possible if the mixing angle satisfies $\sin^2 2\theta_{\mu\tau} \lesssim \text{few} \times 10^{-10}$. This case is simpler because there are then only two important oscillation modes, $\nu_\tau \leftrightarrow \nu_s$ and $\nu_\tau \leftrightarrow \nu_e$. Moreover, these two oscillation modes always have quite different resonance momentum, so that they can each be described by two flavor oscillations. Later (in Sec. IV B) we will consider the alternative case where $\sin^2 2\theta_{\mu\tau} \gtrsim \text{few} \times 10^{-10}$ and $\nu_\tau \leftrightarrow \nu_\mu$ oscillations are also important.

A. Decoupled muon neutrino

If we ignore the muon neutrino, then there are two oscillation modes with approximately the same $|\delta m^2|$, which we denote as $\delta m^2_{\rm large}$:

$$\nu_\tau \leftrightarrow \nu_s, \quad \nu_\tau \leftrightarrow \nu_e. \tag{23}$$

Note that $\delta m^2_{\rm large} \simeq m^2_{\nu_\tau}$ given Eq. (22). We will consider the parameter space region where the δm^2 values of all the other oscillation modes are small enough so that they can be approximately neglected for temperatures $T \gtrsim 0.4$ MeV (this will be true if the δm^2 of these other oscillation modes are all much less than about 1 eV^2). This last condition means that these modes will not significantly affect the neutron/proton ratio and hence cannot significantly affect BBN.

In the following discussion we consider the case $L_{\nu_\tau} > 0$ for definiteness. This means that the $\overline{\nu}_\tau \leftrightarrow \overline{\nu}_s$ generate L_{ν_τ} while $\overline{\nu}_\tau \leftrightarrow \overline{\nu}_e$ oscillations reprocess some of this asymmetry into L_{ν_e}. Note that in this scenario the sign of L_{ν_e} is necessarily the same as the sign of L_{ν_τ}.

The evolution of this system can be described by a straightforward generalization of the two-flavor case given in Eq. (14). In this case there are two MSW resonances, $\overline{\nu}_\tau \leftrightarrow \overline{\nu}_s$ and $\overline{\nu}_\tau \leftrightarrow \overline{\nu}_e$. We denote the resonance momentum of these two oscillations by P_1 and P_2 respectively. They are related to the neutrino asymmetries and temperature through the equations

$$\frac{P_1}{T} = \frac{\delta m^2_{\rm large}}{a_0 T^4 L_1}, \quad \frac{P_2}{T} = \frac{\delta m^2_{\rm large}}{a_0 T^4 L_2}, \tag{24}$$

where $a_0 \equiv 4\sqrt{2}\zeta(3) G_F/\pi^2$ and[10]

$$L_1 \equiv 2L_{\nu_\tau} + L_{\nu_e}, \quad L_2 \equiv L_{\nu_\tau} - L_{\nu_e}. \tag{25}$$

The evolution of the lepton numbers can be obtained by a straightforward generalization to Eqs. (11)–(14):

$$\frac{dL_{\nu_\tau}}{dT} = -X_1 \left| \frac{d(P_1/T)}{dT} \right| - X_2 \left| \frac{d(P_2/T)}{dT} \right|,$$

$$\frac{dL_{\nu_e}}{dT} = X_2 \left| \frac{d(P_2/T)}{dT} \right|,$$

$$\frac{dL_{\nu_\mu}}{dT} = 0, \tag{26}$$

where

$$X_1 \equiv \frac{T}{n_\gamma}[N^-_{\nu_\tau}(P_1) - N^-_{\nu_s}(P_1)],$$

$$X_2 \equiv \frac{T}{n_\gamma}[N^-_{\nu_\tau}(P_2) - N^-_{\nu_e}(P_2)]. \tag{27}$$

Expanding out Eq. (26) we find

$$y_1 \frac{dL_{\nu_\tau}}{dT} = \alpha + \beta \frac{dL_{\nu_e}}{dT},$$

$$y_2 \frac{dL_{\nu_e}}{dT} = \delta + \rho \frac{dL_{\nu_\tau}}{dT}, \tag{28}$$

where

$$y_1 \equiv 1 - f_1 X_1 \frac{\partial(P_1/T)}{\partial L_{\nu_\tau}} - f_2 X_2 \frac{\partial(P_2/T)}{\partial L_{\nu_\tau}}$$

$$= 1 + \frac{2 f_1 X_1 P_1}{T L_1} + \frac{f_2 X_2 P_2}{T L_2},$$

$$y_2 \equiv 1 + f_2 X_2 \frac{\partial(P_2/T)}{\partial L_{\nu_e}} = 1 + \frac{f_2 X_2 P_2}{T L_2},$$

$$\alpha \equiv f_1 X_1 \frac{\partial(P_1/T)}{\partial T} + f_2 X_2 \frac{\partial(P_2/T)}{\partial T}$$

$$= -4 f_1 X_1 P_1/T^2 - 4 f_2 X_2 P_2/T^2,$$

$$\beta \equiv f_1 X_1 \frac{\partial(P_1/T)}{\partial L_{\nu_e}} + f_2 X_2 \frac{\partial(P_2/T)}{\partial L_{\nu_e}}$$

$$= \frac{-f_1 X_1 P_1}{T L_1} + \frac{f_2 X_2 P_2}{T L_2},$$

$$\delta \equiv -f_2 X_2 \frac{\partial(P_2/T)}{\partial T} = 4 f_2 X_2 P_2/T^2,$$

$$\rho \equiv -f_2 X_2 \frac{\partial(P_2/T)}{\partial L_{\nu_\tau}} = \frac{f_2 X_2 P_2}{T L_2}, \tag{29}$$

and $f_i = 1$ for $d(P_i/T)/dt > 0$ and $f_i = -1$ for $d(P_i/T)/dt < 0$ $(i = 1,2)$. Solving Eq. (28) we find

$$\frac{dL_{\nu_\tau}}{dT} = \frac{\delta\beta + y_2\alpha}{y_2 y_1 - \rho\beta},$$

[10] We neglect the L_{ν_μ} asymmetry (and small baryon-electron asymmetries) which is a valid thing to do provided that it is less than about 10^{-5}.

$$\frac{dL_{\nu_e}}{dT} = \frac{\delta + \rho \frac{dL_{\nu_\tau}}{dT}}{y_2}. \quad (30)$$

In order to integrate these equations we need to specify the values of L_{ν_α} (or equivalently P_i/T) at $T = T_c/2$.[11] The high temperature evolution typically does not generate significant L_{ν_e}, i.e. typically $L_{\nu_e} \ll L_{\nu_\tau}$. So we have $P_1/T \sim 0.3, P_2/T \simeq 2P_1/T$.

The evolution of the number densities is treated in a similar fashion to the previous section. Specifically, the MSW transitions effect the adiabatic conversions

$$|\overline{\nu}_\tau\rangle \leftrightarrow |\overline{\nu}_s\rangle, \quad |\overline{\nu}_\tau\rangle \leftrightarrow |\overline{\nu}_e\rangle, \quad (31)$$

at $p = P_1$ and $p = P_2$ respectively. This means that as P_1, P_2 sweeps through the $\overline{\nu}_\tau, \overline{\nu}_e$ momentum distributions,

$$N^-_{\nu_s}(P_1) \to N^-_{\nu_\tau}(P_1),$$

$$N^-_{\nu_\tau}(P_1) \to N^-_{\nu_s}(P_1),$$

$$N^-_{\nu_e}(P_2) \to N^-_{\nu_\tau}(P_2),$$

$$N^-_{\nu_\tau}(P_2) \to N^-_{\nu_e}(P_2). \quad (32)$$

In our numerical work the continuous momentum distribution for each flavor is replaced by a finite number of ''cells'' on a logarithmically spaced mesh. As the momentum P_1, P_2 passes a cell, the number density in the cell is modified according to Eq. (32). Of course weak interactions will repopulate some of these cells as they thermalize the neutrino momentum distributions. We take re-population into account approximately with rate equations of the form of Eq. (17) (for both $\nu_\alpha = \nu_e$ and $\nu_\alpha = \nu_\tau$) and compute the chemical potentials via the procedure discussed in the Appendix.

As in the case of the previous section, the evolution is approximately independent of $\sin^2 2\theta_{\tau s}, \sin^2 2\theta_{\tau e}$ as long as

$$\text{few} \times 10^{-10} \lesssim \sin^2 2\theta_{\tau s} \lesssim \text{few} \times 10^{-5} \left(\frac{\text{eV}^2}{\delta m^2_{\text{large}}} \right)^{1/2},$$

$$\text{few} \times 10^{-10} \lesssim \sin^2 2\theta_{\tau e}, \quad (33)$$

where the lower bound comes from adiabaticity while the upper bound comes from the requirement that $\nu_\tau \leftrightarrow \nu_s$ oscillations do not populate the sterile states at high temperatures before the neutrino asymmetry is initially generated. Of course we have implicitly assumed that the $\nu_e \leftrightarrow \nu_s, \nu_\mu \leftrightarrow \nu_s$ oscillation modes do not significantly populate the sterile neutrinos before BBN. This is a valid assumption for a large range of parmaters even if the ν_s mixes with large mixing angles with ν_μ and/or ν_e. For example, if $\nu_\mu \leftrightarrow \nu_s$ oscillations are approximately maximal with $|\delta m^2_{\mu s}| \simeq 3 \times 10^{-3}$ eV^2 (as suggested by the atmospheric neutrino anomaly), then the $\nu_\mu \leftrightarrow \nu_s$ oscillations can potentially populate the sterile neutrinos at the high temperature $T \approx 8$ MeV. However, this does not happen if the ν_τ is in the eV mass range (for a large range of $\sin^2 2\theta_{\tau s}$) [2,4,6].

In Fig. 4 we plot the evolution of the neutrino asymmetries, L_{ν_τ}, L_{ν_e}, for three examples, $\delta m^2_{\text{large}}/\text{eV}^2 = 0.1, 10, 1000$. As these figures show, for low values of $\delta m^2_{\text{large}}/\text{eV}^2$ the transfer of L_{ν_e} from L_{ν_τ} is not very efficient. This is expected because the transfer of asymmetry relies on the repopulation to distribute the L_{ν_τ} away from the momentum region where it is created (i.e. $p \simeq P_1$) to the momentum region where $\overline{\nu}_\tau \leftrightarrow \overline{\nu}_e$ oscillations are important (i.e. at $p \sim P_2$). As $\delta m^2_{\text{large}}$ increases the temperature where the L_{ν_τ} asymmetry is created increases which makes the transfer to L_{ν_e} more efficient because of the faster repopulation rate.

The implications for BBN are shown in Figs. 5 and 6. Figure 5 treats the $L_{\nu_e} > 0$ case, while Fig. 6 displays the $L_{\nu_e} < 0$ case. As before, our results have a theoretical uncertainty which is dominated by the approximate treatment of repopulation. This uncertainty is expected to be typically less than about $\delta N^{BBN}_{eff} \sim 0.2$ (obviously we expect this uncertainty to be much smaller than this when $\delta_1 N^{BBN}_{eff}$ is small). In the $L_{\nu_\tau} > 0$ case there is a dip at around $\delta m^2 \sim -15$ eV^2. This can be qualitatively understood as follows. For $\delta m^2 \sim -15$ eV^2 the repopulation rate is not so rapid. This has two obvious effects: First, the thermalization of the ν_τ momentum distribution is not so rapid and this would lead to less efficient production of L_{ν_e}. This effect would lead to a decrease in L_{ν_e} (and hence decrease $|\delta N^{BBN}_{eff}|$). Second, the effect of a slow repopulation rate on the ν_e distribution would be expected to have the opposite effect. The reason is that the momentum at which L_{ν_e} creation is most significant is in the high momentum tail. This is because $P_2/T \sim 2P_1/T$ and significant L_{ν_e} is not generated until L_{ν_τ} is sufficiently large, i.e. roughly $P_1/T \gtrsim 2$. The distortion of the ν_e distribution in the high momentum tail greatly enhances the effects for BBN because these effects depend quadratically on the neutrino momentum. Evidently our numerical work indicates that the second effect dominates over the first effect.

Finally, we now consider the more interesting, but more complicated case with the muon neutrino included.

B. Including the muon neutrino

When the muon neutrino is included (i.e. $\sin^2 2\theta_{\mu\tau} \gtrsim$ few $\times 10^{-10}$) there are three oscillation modes with approximately the same $|\delta m^2|$, which we again denote as $\delta m^2_{\text{large}}$:

$$\nu_\tau \leftrightarrow \nu_s, \quad \nu_\tau \leftrightarrow \nu_\mu, \quad \nu_\tau \leftrightarrow \nu_e. \quad (34)$$

All the other oscillation modes have much smaller $|\delta m^2|$ values. As before, we will consider the parameter space region where the δm^2 values of all the other oscillation modes

[11] Of course we also need to specify the initial signs, f_i, which we take as positive. Subsequent evolution does not change these signs.

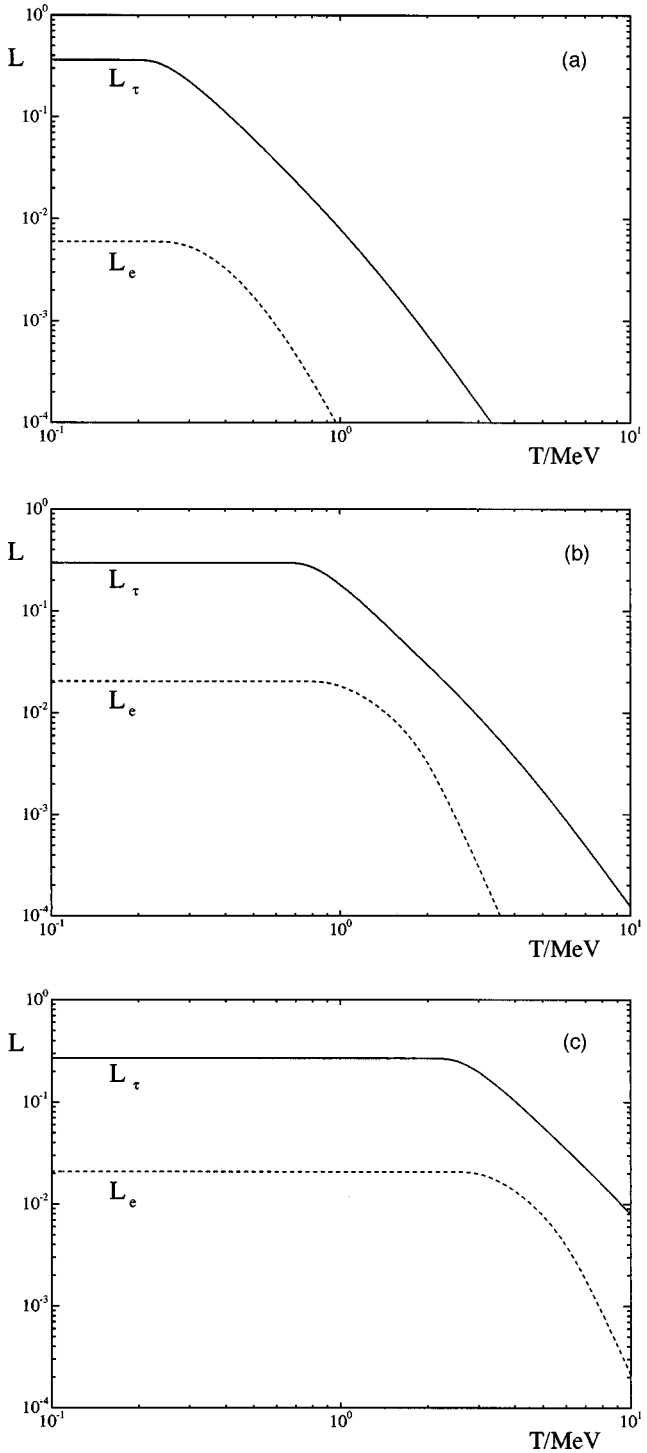

FIG. 4. Low temperature evolution of $L_{\nu_\tau}/h, L_{\nu_e}/h$ ($h \equiv T_\nu^3/T_\gamma^3$) for the model of case 2 (Sec. IV A). (a), (b) and (c) correspond to the parameter choices $\delta m^2_{\rm large}=0.1$ eV^2, $\delta m^2_{\rm large}=10$ eV^2 and $\delta m^2_{\rm large}=1000$ eV^2 respectively.

are small enough so that they can be approximately neglected for temperatures $T \gtrsim 0.4$ MeV. This last condition means that these modes will not affect the neutron/proton ratio and hence cannot significantly affect BBN.

In the following discussion we again consider the case $L_{\nu_\tau} > 0$ for definiteness. This means that the $\overline{\nu}_\tau \leftrightarrow \overline{\nu}_s$ generate

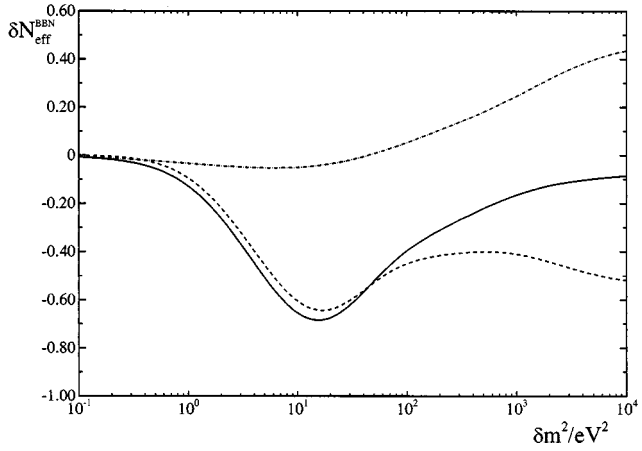

FIG. 5. δN_{eff}^{BBN} versus $\delta m^2_{\rm large}$ for the model of case 2 (Sec. IV A). The dashed line is the contribution $\delta_1 N_{eff}^{BBN}$ due to the effects of the L_{ν_e} asymmetry while the dash-dotted line is the contribution $\delta_2 N_{eff}^{BBN}$ due to the change in the expansion rate. The solid line is the total contribution $\delta N_{eff}^{BBN} = \delta_1 N_{eff}^{BBN} + \delta_2 N_{eff}^{BBN}$. This figure considers the case $L_{\nu_e} > 0$.

L_{ν_τ} while the other two oscillation modes reprocess some of this asymmetry into L_{ν_e}, L_{ν_μ}. In Ref. [3] this system was first considered in this context. There, it was assumed that $L_{\nu_e} = L_{\nu_\mu}$. While this is a good approximation for large enough values of $|\delta m^2|$, it is not always valid (as we will show below). In the following we will not assume this and consider the effect of the three oscillation modes.

At this point one may legitimately worry about 3-flavor effects. This is because the resonance momentum of the $\nu_\tau \leftrightarrow \nu_e$ and $\nu_\tau \leftrightarrow \nu_\mu$ oscillation modes are expected to be approximately equal. However, it turns out that these oscillations tend to be dynamically driven apart as we will explain later on. Thus, it turns out that it is actually reasonable to treat all three oscillation modes independently as 2-flavor MSW transitions. In the earlier paper [3] this issue was not fully discussed, so our treatment here improves on Ref. [3].

In this system there are three MSW resonances, $\overline{\nu}_\tau \leftrightarrow \overline{\nu}_s$, $\overline{\nu}_\tau \leftrightarrow \overline{\nu}_\mu$ and $\overline{\nu}_\tau \leftrightarrow \overline{\nu}_e$. We denote the resonance momentum

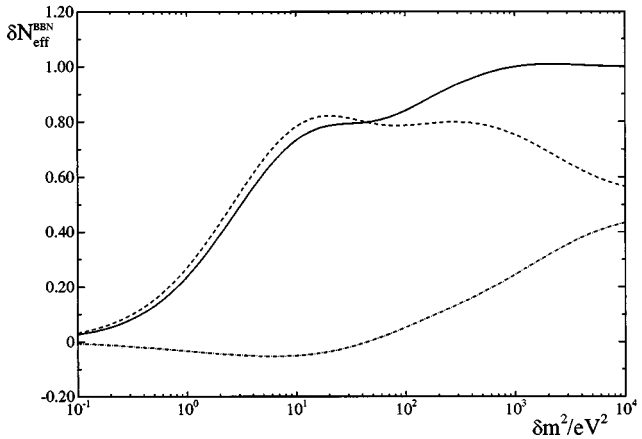

FIG. 6. Same as Fig. 5 except $L_{\nu_e} < 0$ is considered.

of these three oscillations by P_1, P_2 and P_3 respectively. They are related to the neutrino asymmetries and temperature through the equations

$$\frac{P_i}{T} = \frac{\delta m^2_{\rm large}}{a_0 T^4 L_i}, \tag{35}$$

where $i=1,2,3$, $a_0 \equiv 4\sqrt{2}\zeta(3) G_F/\pi^2$ and

$$L_1 \equiv 2L_{\nu_\tau} + L_{\nu_\mu} + L_{\nu_e}, \quad L_2 \equiv L_{\nu_\tau} - L_{\nu_\mu}, \quad L_3 \equiv L_{\nu_\tau} - L_{\nu_e}. \tag{36}$$

Using a similar procedure to the previous (sub)sections, we have

$$\frac{dL_{\nu_\tau}}{dT} = -X_1\left|\frac{d(P_1/T)}{dT}\right| - X_2\left|\frac{d(P_2/T)}{dT}\right| - X_3\left|\frac{d(P_3/T)}{dT}\right|,$$

$$\frac{dL_{\nu_e}}{dT} = X_3\left|\frac{d(P_3/T)}{dT}\right|,$$

$$\frac{dL_{\nu_\mu}}{dT} = X_2\left|\frac{d(P_2/T)}{dT}\right|, \tag{37}$$

where

$$X_1 \equiv \frac{T}{n_\gamma}[N^-_{\nu_\tau}(P_1) - N^-_{\nu_s}(P_1)],$$

$$X_2 \equiv \frac{T}{n_\gamma}[N^-_{\nu_\tau}(P_2) - N^-_{\nu_\mu}(P_2)],$$

$$X_3 \equiv \frac{T}{n_\gamma}[N^-_{\nu_\tau}(P_3) - N^-_{\nu_e}(P_3)]. \tag{38}$$

Expanding out Eq. (37) we find

$$y_1\frac{dL_{\nu_\tau}}{dT} = \alpha + \beta\frac{dL_{\nu_e}}{dT} + \gamma\frac{dL_{\nu_\mu}}{dT},$$

$$y_2\frac{dL_{\nu_e}}{dT} = \delta + \rho\frac{dL_{\nu_\tau}}{dT},$$

$$y_3\frac{dL_{\nu_\mu}}{dT} = \eta + \phi\frac{dL_{\nu_\tau}}{dT}, \tag{39}$$

where

$$y_1 \equiv 1 - f_1X_1\frac{\partial(P_1/T)}{\partial L_{\nu_\tau}} - f_2X_2\frac{\partial(P_2/T)}{\partial L_{\nu_\tau}} - f_3X_3\frac{\partial(P_3/T)}{\partial L_{\nu_\tau}}$$

$$= 1 + \frac{2f_1X_1P_1}{TL_1} + \frac{f_2X_2P_2}{TL_2} + \frac{f_3X_3P_3}{TL_3},$$

$$y_2 \equiv 1 + f_3X_3\frac{\partial(P_3/T)}{\partial L_{\nu_e}} = 1 + \frac{f_3X_3P_3}{TL_3},$$

$$y_3 \equiv 1 + f_2X_2\frac{\partial(P_2/T)}{\partial L_{\nu_\mu}} = 1 + \frac{f_2X_2P_2}{TL_2},$$

$$\alpha \equiv f_1X_1\frac{\partial(P_1/T)}{\partial T} + f_2X_2\frac{\partial(P_2/T)}{\partial T} + f_3X_3\frac{\partial(P_3/T)}{\partial T}$$

$$= -4f_1X_1P_1/T^2 - 4f_2X_2P_2/T^2 - 4f_3X_3P_3/T^2,$$

$$\beta \equiv f_1X_1\frac{\partial(P_1/T)}{\partial L_{\nu_e}} + f_3X_3\frac{\partial(P_3/T)}{\partial L_{\nu_e}}$$

$$= \frac{-f_1X_1P_1}{TL_1} + \frac{f_3X_3P_3}{TL_3},$$

$$\gamma \equiv f_1X_1\frac{\partial(P_1/T)}{\partial L_{\nu_\mu}} + f_2X_2\frac{\partial(P_2/T)}{\partial L_{\nu_\mu}}$$

$$= \frac{-f_1X_1P_1}{TL_1} + \frac{f_2X_2P_2}{TL_2},$$

$$\delta \equiv -f_3X_3\frac{\partial(P_3/T)}{\partial T} = 4f_3X_3P_3/T^2,$$

$$\rho \equiv -f_3X_3\frac{\partial(P_3/T)}{\partial L_{\nu_\tau}} = \frac{f_3X_3P_3}{TL_3},$$

$$\eta \equiv -f_2X_2\frac{\partial(P_2/T)}{\partial T} = 4f_2X_2P_2/T^2,$$

$$\phi \equiv -f_2X_2\frac{\partial(P_2/T)}{\partial L_{\nu_\tau}} = \frac{f_2X_2P_2}{TL_2}, \tag{40}$$

and $f_i=1$ for $d(P_i/T)/dt>0$ and $f_i=-1$ for $d(P_i/T)/dt<0$ $(i=1,2,3)$. Solving Eq. (39) we find

$$\frac{dL_{\nu_e}}{dT} = \frac{\delta y_3(y_1y_3 - \gamma\phi) + \rho y_3(\alpha y_3 + \gamma\eta)}{y_2y_3(y_1y_3 - \gamma\phi) - \rho\beta y_3^2},$$

$$\frac{dL_{\nu_\tau}}{dT} = \frac{\alpha y_3 + \gamma\eta + \beta y_3\dfrac{dL_{\nu_e}}{dT}}{y_1y_3 - \gamma\phi},$$

$$\frac{dL_{\nu_\mu}}{dT} = \frac{1}{y_3}\left[\eta + \phi\frac{dL_{\nu_\tau}}{dT}\right]. \tag{41}$$

In order to integrate these equations we need to specify the values of L_{ν_α} (or equivalently P_i/T) at $T=T_c/2$. The high temperature evolution typically does not generate significant L_{ν_e}, L_{ν_μ} (i.e. typically $L_{\nu_e}, L_{\nu_\mu} \ll L_{\nu_\tau}$). So we have $P_1/T \sim 0.3, P_2/T \simeq P_3/T \simeq 2P_1/T$. Now, there is no reason why P_2/T should exactly coincide with P_3/T (although it will be approximately equal). In fact for these two oscillations, $P_2/T = P_3/T$ is not dynamically stable as we shall now ex-

plain. The behavior of oscillations such as these (in the context of a quite different model) has been studied in some detail in Ref. [9]. Generically there are two possible outcomes. Either the evolution of lepton number is such that it drives $P_2/T \to P_3/T$ *or* the evolution of lepton numbers is such as to drive them apart. To figure out what is going to happen imagine that P_2/T is slightly less than P_3/T. In other words the $\overline{\nu}_\tau \leftrightarrow \overline{\nu}_e$ oscillation resonance preceeds the $\overline{\nu}_\tau \leftrightarrow \overline{\nu}_\mu$ oscillation resonance. This means that the $\overline{\nu}_\tau \leftrightarrow \overline{\nu}_e$ resonance will efficiently interchange $\overline{\nu}_\tau$ and $\overline{\nu}_e$ states at the resonance. This will transfer some L_{ν_τ} to L_{ν_e} and will thus speed up the resonance a bit since it is inversely proportional to the difference of L_{ν_τ} and L_{ν_e}. The trailing $\overline{\nu}_\tau \leftrightarrow \overline{\nu}_\mu$ resonance will be less effective in transferring L_{ν_τ} to L_{ν_μ} because at this resonance there will be approximately equal number of $\overline{\nu}_\mu$ and $\overline{\nu}_\tau$ states thanks to the efforts of the $\overline{\nu}_\tau \leftrightarrow \overline{\nu}_e$ resonance. Thus the two resonances will slowly move apart until eventually they will be far enough apart so that the thermalization due to the collisions will be rapid enough to thermalize the ν_τ spectrum such that the L_{ν_μ} is created at approximately the same rate as the L_{ν_e}. For definiteness, we will assume as our initial condition that $P_3/T > P_2/T$. For our numerical work we will assume that $P_3/T = 1.01 P_2/T$ initially. This could be due to a slightly larger $|\delta m^2_{\tau e}| > |\delta m^2_{\tau\mu}|$ for example. We found very similar results for even smaller choices such as $P_3/T = 1.001 P_2/T$.

It is straightforward to numerically integrate the evolution equations (41) with $T = T_c/2$ ''initial conditions'' as described above. We keep track of the number distributions of all 4 flavors (using a completely analogous procedure to the previous cases). In Fig. 7 we plot the evolution of the neutrino asymmetries, $L_{\nu_\tau}, L_{\nu_\mu}, L_{\nu_e}$, for three examples, $\delta m^2_{\rm large}/{\rm eV}^2 = 0.1, 10, 1000$. The implications for BBN are shown in Figs. 8 and 9. Figure 8 treats the $L_{\nu_e} > 0$ case, while Fig. 9 displays the $L_{\nu_e} < 0$ case. As these figures show, this case is very similar to the previous results where the muon neutrino was neglected. Of course if we had started with $P_2/T > P_3/T$, then the L_{ν_μ} and L_{ν_e} are approximately interchanged. In this case, the modification to N^{BBN}_{eff} would be somewhat smaller, especially for lower values of $\delta m^2_{\rm large}$.

Let us compare our results with the original work in Ref. [3] and the more recent work of Ref. [10]. In Ref. [3] we made the approximation that the repopulation was instantaneous above about 1.5 MeV. We also assumed that $L_{\nu_e} = L_{\nu_\mu}$ and derived evolution equations consistent with that assumption. We found that $\delta N^{BBN}_{eff} \approx -0.5$ for $L_{\nu_e} > 0$ and $\delta N^{BBN}_{eff} \approx 0.4$ for $L_{\nu_e} < 0$ for

$$10 \lesssim \delta m^2_{\rm large}/{\rm eV}^2 \lesssim 1000. \tag{42}$$

For the $L_{\nu_e} > 0$ case the results are in rough agreement for $\delta m^2_{\rm large} \lesssim 100$ eV^2. The difference for larger $\delta m^2_{\rm large}$ is due to the more accurate treatment of chemical decoupling which suggests a lower decoupling temperature. For the $L_{\nu_e} < 0$ case the effect is underestimated by about 0.4 in δN^{BBN}_{eff} in Ref. [3]. This difference is partly due to a mistake in the numerical work of Ref. [3] which we have recently discovered.

In Ref. [10] they consider the case of Sec. IV A of this

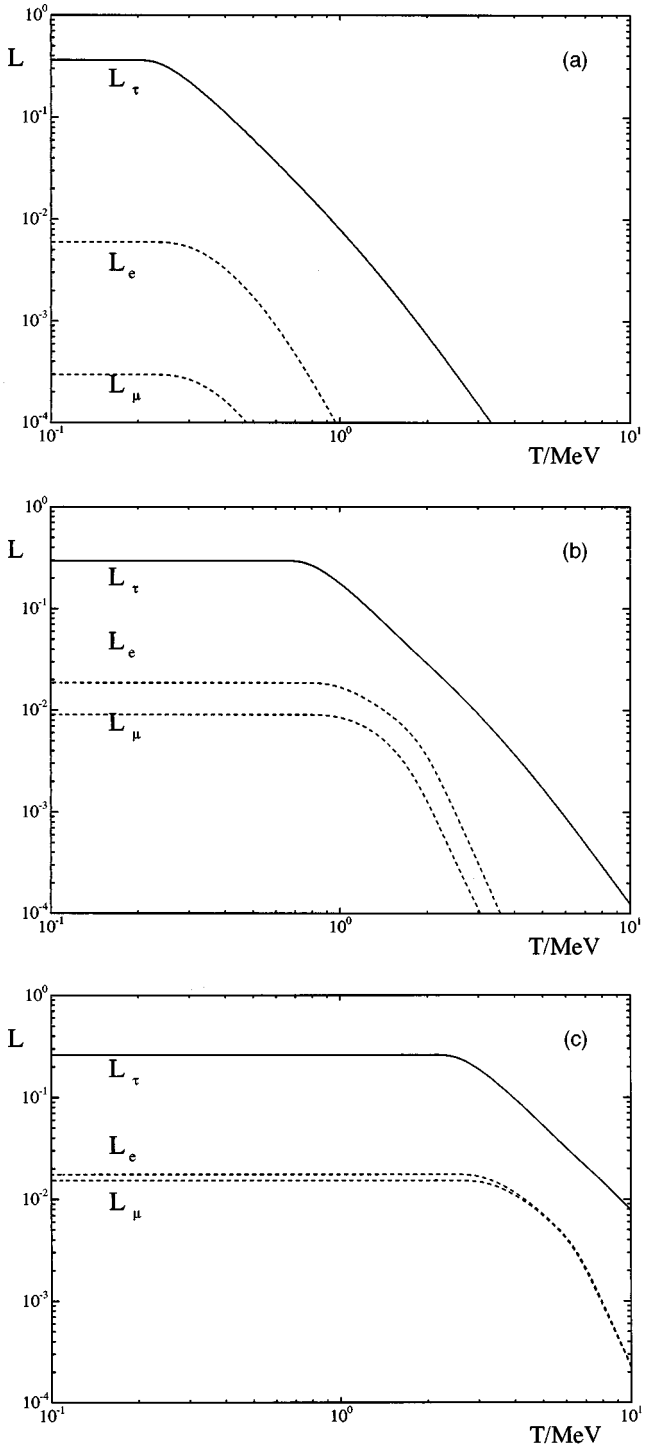

FIG. 7. Low temperature evolution of $L_{\nu_\tau}/h, L_{\nu_\mu}/h, L_{\nu_e}/h$ ($h \equiv T_\nu^3/T_\gamma^3$) for the model of case 2 (Sec. IV B). (a), (b), and (c) correspond to the parameter choices $\delta m^2_{\rm large} = 0.1$ eV^2, $\delta m^2_{\rm large} = 10$ eV^2 and $\delta m^2_{\rm large} = 1000$ eV^2 respectively.

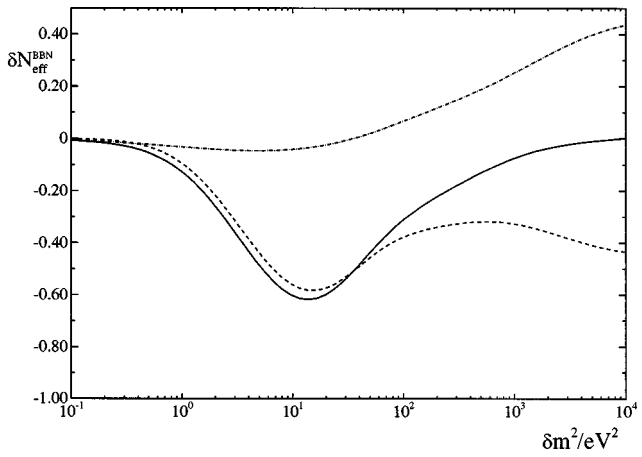

FIG. 8. δN_{eff}^{BBN} versus $\delta m^2_{\rm large}$ for the model of case 2 (Sec. IV B). The dashed line is the contribution $\delta_1 N_{eff}^{BBN}$ due to the effects of the L_{ν_e} asymmetry while the dash-dotted line is the contribution $\delta_2 N_{eff}^{BBN}$ due to the change in the expansion rate. The solid line is the total contribution $\delta N_{eff}^{BBN} = \delta_1 N_{eff}^{BBN} + \delta_2 N_{eff}^{BBN}$. This figure considers the case $L_{\nu_e} > 0$.

section, i.e. neglecting the muon neutrino. Their results do not seem to be consistent with ours, expecially for $L_{\nu_e} > 0$. We do not know the reason for this.

V. CONCLUSION

We have made a detailed study of several ''four neutrino scenarios'' which can generate significant L_{ν_e} asymmetry, thereby affecting BBN (these scenarios were first discussed in this context in Ref. [3]). In the first case we considered the direct production of L_{ν_e} from $\nu_e \leftrightarrow \nu_s$ oscillations. Our results are shown in Figs. 2 and 3. Clearly very large modifications to BBN are possible and depend sensitively on δm^2 [but are approximately independent of $\sin^2 2\theta$ as long as $\sin^2 2\theta$ is in the range, Eq. (7)]. The results also depend critically on the sign of L_{ν_e}. We also studied the indirect production of L_{ν_e} from L_{ν_τ}. Our results are given in Figs. 5 and 6 for the case where the muon neutrino can be neglected and Figs. 8 and 9 where the muon neutrino is included. These results are in rough agreement with our earlier conclusion [3] that $\delta N_{eff}^{BBN} \sim -0.5$ for the case of positive L_{ν_e} for the parameter range, Eq. (42). Notice that the figures show a slightly larger effect for $\delta m^2 \sim 10\ {\rm eV}^2$ where the slow repopulation rate becomes important (Ref. [3] assumed that repopulation was instantaneous). Also the more accurate treatment of repopulation in the kinetic decoupling region suggests a larger δN_{eff}^{BBN} for $|\delta m^2|/{\rm eV}^2 \gtrsim 100$ than was found previously.

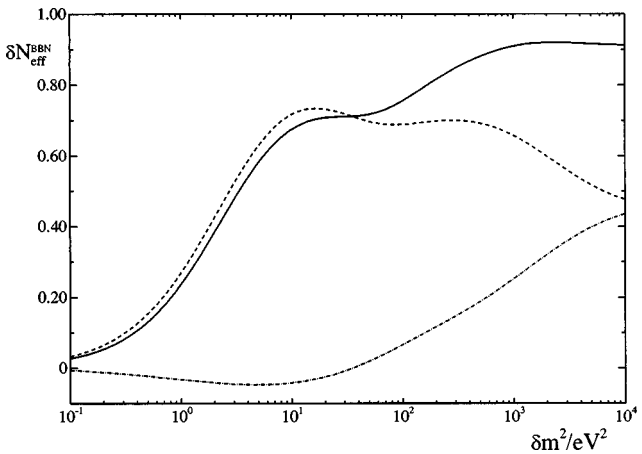

FIG. 9. Same as Fig. 8 except $L_{\nu_e} < 0$ is considered.

We conclude by emphasizing once more that the detailed predictions of models with light sterile neutrinos are quite model dependent. Quantitatively different results occur for four neutrino models with approximately degenerate ν_μ, ν_τ [7], as well as in six neutrino models with three light sterile neutrinos approximately maximally mixed with each of the ordinary neutrinos [9]. It is a remarkable prospect that accurate determinations of the primordial element abundances, as well as forthcoming precision measurements of the anisotropy of the cosmic microwave background, may one day help to distinguish between competing models of particle physics.

ACKNOWLEDGMENTS

The author thanks R. R. Volkas and T. L. Yoon for comments.

APPENDIX: REPOPULATION

Consider for definiteness the case of $\overline{\nu}_\alpha \leftrightarrow \overline{\nu}_s$ oscillations which generate a large L_{ν_α}. The $\overline{\nu}_\alpha \leftrightarrow \overline{\nu}_s$ oscillations depelete the $\overline{\nu}_\alpha$ states at the MSW resonance. Elastic collisions will tend to thermalize the momentum distributions so that they can be approximately described by chemical potentials, while inelastic collisions will create and modify the chemical potentials. Let us denote the total elastic and inelastic collision rates by the notation $\Gamma^E_\alpha, \Gamma^I_\alpha$ respectively. It happens that $\Gamma^E_\alpha \gg \Gamma^I_\alpha$,[12] so it makes sense to describe the neutrino distributions in terms of chemical potentials and a common temperature throughout the chemical decoupling period ($2 \lesssim T/{\rm MeV} \lesssim 4$). *We emphasize that the actual momentum distribution is always computed from Eq. (17); the purpose of this present discussion is to work out the evolution of the chemical potentials which are needed on the right-hand side of Eq. (17).*

The chemical potentials are related to the lepton number by the equation

$$L_{\nu_\alpha} = \frac{1}{4\zeta(3)} \int_0^\infty \frac{x^2 dx}{1 + e^{x + \tilde{\mu}_\alpha}} - \frac{1}{4\zeta(3)} \int_0^\infty \frac{x^2 dx}{1 + e^{x + \tilde{\mu}_{\overline{\alpha}}}}, \tag{A1}$$

[12] Numerically $\Gamma^E_e/\Gamma^I_e \simeq 6.3$, $\Gamma^E_{\mu,\tau}/\Gamma^I_{\mu,\tau} \simeq 8.0$.

TABLE I. Inelastic processes together with their thermally averaged interaction rates.

Process	Rate
(1) $\nu_\tau\bar{\nu}_\tau \leftrightarrow \nu_\mu\bar{\nu}_\mu$	$\Gamma_1^I = F_0$
(2) $\nu_\tau\bar{\nu}_\tau \leftrightarrow \nu_e\bar{\nu}_e$	$\Gamma_2^I = F_0$
(3) $\nu_\tau\bar{\nu}_\tau \leftrightarrow e^+e^-$	$\Gamma_3^I = (8x^2-4x+1)F_0$
(4) $\nu_\mu\bar{\nu}_\mu \leftrightarrow \nu_e\bar{\nu}_e$	$\Gamma_4^I = F_0$
(5) $\nu_\mu\bar{\nu}_\mu \leftrightarrow e^+e^-$	$\Gamma_5^I = (8x^2-4x+1)F_0$
(6) $\nu_e\bar{\nu}_e \leftrightarrow e^+e^-$	$\Gamma_6^I = (8x^2+4x+1)F_0$

where $\tilde{\mu}_\alpha \equiv \mu_{\nu_\alpha}/T$, $\tilde{\mu}_{\bar{\alpha}} \equiv \mu_{\bar{\nu}_\alpha}/T$ and $\zeta(3) \simeq 1.202$ is the Riemann zeta function of 3. Expanding out the above equation,

$$L_{\nu_\alpha} \simeq -\frac{1}{24\zeta(3)}[\pi^2(\tilde{\mu}_\alpha - \tilde{\mu}_{\bar{\alpha}}) - 6(\tilde{\mu}_\alpha^2 - \tilde{\mu}_{\bar{\alpha}}^2)\ln 2 + (\tilde{\mu}_\alpha^3 - \tilde{\mu}_{\bar{\alpha}}^3)]. \tag{A2}$$

This is an exact equation for $\tilde{\mu}_\alpha = -\tilde{\mu}_{\bar{\alpha}}$; otherwise it holds to a good approximation provided that $|\tilde{\mu}_{\alpha,\bar{\alpha}}| \lesssim 1$. If we turn off inelastic collisions for a moment, and assume that the oscillation generated L_{ν_α} is positive, then the oscillations generate a large $\tilde{\mu}_{\bar{\alpha}}$. The evolution of $\tilde{\mu}_{\bar{\alpha}}$ due to the generation of L_{ν_α} (i.e. due to oscillations) can easily be obtained from Eq. (A2),

$$\left.\frac{d\tilde{\mu}_{\bar{\alpha}}}{dT}\right|_{osc} \simeq \left[\frac{24\zeta(3)}{\pi^2 - 12\tilde{\mu}_{\bar{\alpha}}\ln 2 + 3\tilde{\mu}_{\bar{\alpha}}^2}\right]\frac{dL_{\nu_\alpha}}{dT}, \quad \left.\frac{d\tilde{\mu}_\alpha}{dT}\right|_{osc} \simeq 0. \tag{A3}$$

Now, let us turn on the inelastic collisions and see what happens. There are six inelastic processes, which we list in Table I together with their thermally averaged interaction rates [20].

In the above table, $x \equiv \sin^2\theta_w$ is the weak mixing angle ($\sin^2\theta_w \simeq 0.23$), and $F_0 \equiv (G_F^2\langle p\rangle^2/6\pi)\, n_\gamma \simeq 0.13 G_F^2 T^5$. Consider the first process listed in the above table. This process will change the number of $\nu_\tau, \bar{\nu}_\tau, \nu_\mu, \bar{\nu}_\mu$ states such that

$$\left.\frac{dn_{\nu_\tau}}{dt}\right|_{(1)} = \left.\frac{dn_{\bar{\nu}_\tau}}{dt}\right|_{(1)} = -\left.\frac{dn_{\nu_\mu}}{dt}\right|_{(1)} = -\left.\frac{dn_{\bar{\nu}_\mu}}{dt}\right|_{(1)}, \tag{A4}$$

where the subscript ''$|_{(1)}$'' denotes the contribution to the rate of change due to the process (1) in the table. The rate can be expressed approximately as follows:

$$\left.\frac{d(n_{\nu_\tau}/n_0)}{dt}\right|_{(1)} = \frac{1}{n_0}\int_0^\infty\int_0^\infty [N_{\nu_\mu}(p)N_{\bar{\nu}_\mu}(p') - N_{\nu_\tau}(p)N_{\bar{\nu}_\tau}(p')]\sigma_1(p,p')dpdp'. \tag{A5}$$

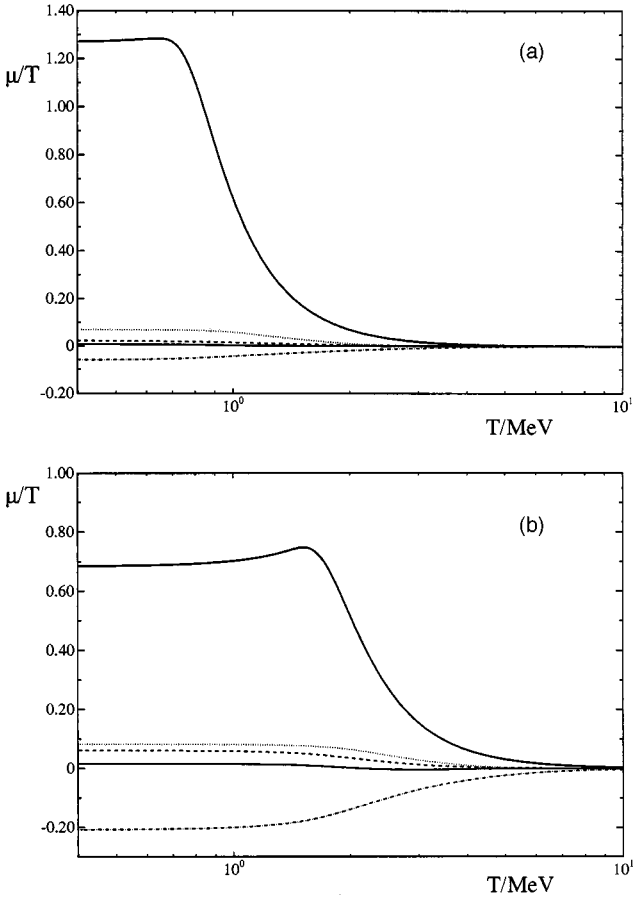

FIG. 10. Evolution of $\tilde{\mu}_{\alpha,\bar{\alpha}}$ for the model of case 2 (Sec. IV A). (a) and (b) correspond to the parameter choices $\delta m^2_{\rm large} = 10$ eV^2 and $\delta m^2_{\rm large} = 200$ eV^2 respectively. In the figures the thin solid, dashed, dash-dotted, dotted and thick solid lines correspond to $\tilde{\mu}_e, \tilde{\mu}_\mu, \tilde{\mu}_\tau, \tilde{\mu}_{\bar{e}}$ and $\tilde{\mu}_{\bar{\tau}}$ respectively. Note that $\tilde{\mu}_{\bar{\mu}} = \tilde{\mu}_\mu$ in this case.

For convenience we have normalized with respect to the number of neutrinos in a Fermi-Dirac distribution with zero chemical potential, $n_0 = 3\zeta(3)T^3/4\pi^2$. Let us further make the useful approximation that

$$N_{\nu_\alpha}(p) \simeq e^{-\tilde{\mu}_\alpha}N_0(p), \quad N_{\bar{\nu}_\alpha}(p) \simeq e^{-\tilde{\mu}_{\bar{\alpha}}}N_0(p), \quad N_{e^\pm}(p) = N_0(p), \tag{A6}$$

where $N_0(p)$ is the Fermi-Dirac distribution with zero chemical potential. Note that the $e^\pm$ distributions have zero chemical potential due to the very rapid collisions with the background photons (see e.g. Ref [13]). Thus, with the above approximation, Eq. (A5) can be expressed in the simple form

$$\left.\frac{d\eta_{\nu_\tau}}{dt}\right|_{(1)} = (\eta_{\nu_\mu}\eta_{\bar{\nu}_\mu} - \eta_{\nu_\tau}\eta_{\bar{\nu}_\tau})\Gamma_1^I, \tag{A7}$$

where $\eta_{\nu_\alpha} \equiv e^{\tilde{\mu}_\alpha}$, $\eta_{\bar{\nu}_\alpha} \equiv e^{\tilde{\mu}_{\bar{\alpha}}}$. Clearly, we also have that

$$\left.\frac{d\eta_{\nu_\tau}}{dt}\right|_{(1)} = \left.\frac{d\eta_{\nu_\tau}^-}{dt}\right|_{(1)} = -\left.\frac{d\eta_{\nu_\mu}}{dt}\right|_{(1)} = -\left.\frac{d\eta_{\nu_\mu}^-}{dt}\right|_{(1)},$$

$$\left.\frac{d\eta_{\nu_e}}{dt}\right|_{(1)} = \left.\frac{d\eta_{\nu_e}^-}{dt}\right|_{(1)} = 0. \quad \text{(A8)}$$

A similar set of equations can be obtained for the other five inelastic processes. Putting this altogether, we have

$$\left.\frac{d\eta_{\nu_\tau}}{dt}\right|_{repop} = \left.\frac{d\eta_{\nu_\tau}^-}{dt}\right|_{repop} = \sum_{i=1}^{6}\left.\frac{d\eta_{\nu_\tau}}{dt}\right|_{(i)}$$

$$= (\eta_{\nu_\mu}\eta_{\nu_\mu}^- - \eta_{\nu_\tau}\eta_{\nu_\tau}^-)\Gamma_1^I + (\eta_{\nu_e}\eta_{\nu_e}^- - \eta_{\nu_\tau}\eta_{\nu_\tau}^-)\Gamma_2^I + (1-\eta_{\nu_\tau}\eta_{\nu_\tau}^-)\Gamma_3^I,$$

$$\left.\frac{d\eta_{\nu_\mu}}{dt}\right|_{repop} = \left.\frac{d\eta_{\nu_\mu}^-}{dt}\right|_{repop} = \sum_{i=1}^{6}\left.\frac{d\eta_{\nu_\mu}}{dt}\right|_{(i)}$$

$$= (\eta_{\nu_\tau}\eta_{\nu_\tau}^- - \eta_{\nu_\mu}\eta_{\nu_\mu}^-)\Gamma_1^I + (\eta_{\nu_e}\eta_{\nu_e}^- - \eta_{\nu_\mu}\eta_{\nu_\mu}^-)\Gamma_4^I + (1-\eta_{\nu_\mu}\eta_{\nu_\mu}^-)\Gamma_5^I,$$

$$\left.\frac{d\eta_{\nu_e}}{dt}\right|_{repop} = \left.\frac{d\eta_{\nu_e}^-}{dt}\right|_{repop} = \sum_{i=1}^{6}\left.\frac{d\eta_{\nu_e}}{dt}\right|_{(i)}$$

$$= (\eta_{\nu_\tau}\eta_{\nu_\tau}^- - \eta_{\nu_e}\eta_{\nu_e}^-)\Gamma_2^I + (\eta_{\nu_\mu}\eta_{\nu_\mu}^- - \eta_{\nu_e}\eta_{\nu_e}^-)\Gamma_4^I + (1-\eta_{\nu_e}\eta_{\nu_e}^-)\Gamma_6^I. \quad \text{(A9)}$$

Of course the total rate of change of $\tilde{\mu}_\alpha, \tilde{\mu}_{\bar{\alpha}}$ is given by

$$\left.\frac{d\tilde{\mu}_\alpha}{dt}\right| = \left.\frac{d\tilde{\mu}_\alpha}{dt}\right|_{osc} + \left.\frac{d\tilde{\mu}_\alpha}{dt}\right|_{repop},$$

$$\left.\frac{d\tilde{\mu}_{\bar{\alpha}}}{dt}\right| = \left.\frac{d\tilde{\mu}_{\bar{\alpha}}}{dt}\right|_{osc} + \left.\frac{d\tilde{\mu}_{\bar{\alpha}}}{dt}\right|_{repop}. \quad \text{(A10)}$$

The above equations can be used to approximately compute the set of chemical potentials. Then using Eqs. (17) the evolution of the set of number distributions can be obtained.

In Fig. 10 we give the evolution of $\tilde{\mu}_{\alpha,\bar{\alpha}}$ for some illustrative examples. In the figure we consider the model discussed in Sec. IV A with the parameter choice $\delta m^2_{\rm large} = 10\ {\rm eV}^2$ for Fig. 10(a) and $\delta m^2_{\rm large} = 200\ {\rm eV}^2$ for Fig. 10(b).

We have also compared the above repopulation procedure with the simpler procedure of a fixed decoupling temperature, T^α_{dec}, where $\mu_{\nu_\alpha} = -\mu_{\nu_\alpha}^-$ for $T > T^\alpha_{dec}$ and μ_{ν_α} frozen (in the case $L_{\nu_\alpha} > 0$) for $T < T^\alpha_{dec}$. We get rough agreement provided that $T^\alpha_{dec} \approx 3$ MeV.

[1] R. Foot, M.J. Thomson, and R.R. Volkas, Phys. Rev. D **53**, 5349 (1996).
[2] R. Foot and R.R. Volkas, Phys. Rev. D **55**, 5147 (1997).
[3] R. Foot and R.R. Volkas, Phys. Rev. D **56**, 6653 (1997); **59**, 029901(E) (1999).
[4] R. Foot, Astropart. Phys. **10**, 253 (1999).
[5] N.F. Bell, R.R. Volkas, and Y.Y.Y. Wong, Phys. Rev. D **59**, 113001 (1999).
[6] P. Di Bari, P. Lipari, and M. Lusignoli, hep-ph/9907548.
[7] N.F. Bell, R. Foot, and R.R. Volkas, Phys. Rev. D **58**, 105010 (1998).
[8] R. Foot and R.R. Volkas, Astropart. Phys. **7**, 283 (1997).
[9] R. Foot and R.R. Volkas, Phys. Rev. D (to be published), hep-ph/9904336, 1999.
[10] X. Shi, G.M. Fuller, and K. Abazajian, Phys. Rev. D **60**, 063002 (1999).
[11] For some recent studies, see e.g. N. Hata *et al.*, Phys. Rev. Lett. **75**, 3977 (1995); P.J. Kernan and S. Sarkar, Phys. Rev. D **54**, 3681 (1996); K.A. Olive and D. Thomas, Astropart. Phys. **11**, 403 (1999); S. Burles *et al.*, Phys. Rev. Lett. **82**, 4176 (1999); E. Lisi *et al.*, Phys. Rev. D **59**, 123520 (1999).
[12] See, for example, K. Kainulainen, H. Kurki-Suonio, and E. Sihvola, Phys. Rev. D **59**, 083505 (1999).
[13] S. Weinberg, *Gravitation and Cosmology* (Wiley, New York, 1972), Chap. 15.
[14] K.A. Olive, D.N. Schramm, D. Thomas, and T.P. Walker, Phys. Lett. B **265**, 239 (1991).
[15] T.P. Walker *et al.*, Astrophys. J. **376**, 51 (1991).
[16] R. Barbieri and A. Dolgov, Nucl. Phys. **B349**, 743 (1991); K. Enqvist, K. Kainulainen, and J. Maalampi, *ibid.* **B349**, 754 (1991).
[17] D.P. Kirilova and M.V. Chizhov, Phys. Lett. B **393**, 375 (1997); Phys. Rev. D **58**, 073004 (1998).
[18] R.A. Harris and L. Stodolsky, Phys. Lett. **116B**, 464 (1982); **78B**, 313 (1978); A. Dolgov, Sov. J. Nucl. Phys. **33**, 700 (1981); L. Stodolsky, Phys. Rev. D **36**, 2273 (1987); D. Notzold and G. Raffelt, Nucl. Phys. **B307**, 924 (1988); P. Langacker, University of Pennsylvania Report No. UPR 0401T, 1989; R. Barbieri and A. Dolgov, Phys. Lett. B **237**, 440 (1990); K. Kainulainen, *ibid.* **244**, 191 (1990); M. Thomson, Phys. Rev. A **45**, 2243 (1991); K. Enqvist, K. Kainulainen, and J. Maalampi, Phys. Lett. B **244**, 186 (1991); K. Enqvist, K. Kainulainen, and M. Thomson, Nucl. Phys. **B373**, 498 (1992); J. Cline, Phys. Rev. Lett. **68**, 3137 (1992); X. Shi, D.N. Schramm, and B.D. Fields, Phys. Rev. D **48**, 2563 (1993); G. Raffelt, G. Sigl, and L. Stodolsky, Phys. Rev. Lett. **70**, 2363 (1993); B.H.J. McKellar and M.J. Thomson, Phys. Rev. D **49**, 2710 (1994); R. Foot and R.R. Volkas, Phys. Rev. Lett. **75**, 4350 (1995).
[19] Particle Data Group, C. Caso *et al.*, Eur. Phys. J. C **3**, 1 (1998).
[20] See the paper by Enqvist, Kainulainen, and Thomson [18].
[21] R.E. Lopez, S. Dodelson, A. Heckler, and M.S. Turner, Phys. Rev. Lett. **82**, 3952 (1999); S. Hannestad and G. Raffelt, Phys. Rev. D **59**, 043001 (1999).
[22] K. Enqvist, K. Kainulainen, and A. Sorri, hep-ph/9906452.
[23] X. Shi, Phys. Rev. D **54**, 2753 (1996).
[24] P. DiBari, hep-ph/9911214..